Fermi Gases and Fermi Liquids

Tristan.W

December 30, 2025

Contents

1 Fermi Distribution in the Uniform Ideal Fermi Gas **3**
- 1.1 Fermi sea, occupation numbers, and excitations . . . 3
- 1.2 Fermi–Dirac distribution, classical limit, and kinetic energy . . . 4
- 1.3 External Potential and Local density approximation(LDA) . . . 6
- 1.4 Example: Harmonic Trap . . . 7
- 1.5 Time-of-flight (TOF): momentum distribution and aspect ratio . . . 8

2 Quantized Conductance through a Quantum Point Contact **8**
- 2.1 Two-terminal setup and the Landauer–Büttiker formula . . . 9
- 2.2 QPC design and semiclassical channel picture . . . 10
- 2.3 Conductance quantization . . . 11

3 Landau Fermi Liquid: Quasiparticles, m^*, Z, and Self-Energy **12**
- 3.1 Core assumptions and the role of the Fermi surface . . . 12
- 3.2 Why quasi-particles exist . . . 12
- 3.3 Higher-order structure: quasiparticle interactions and Landau parameters . . . 14
- 3.4 Domain of validity and possible fates of interacting Fermi systems . . . 14
- 3.5 Self-energy and the Fermi polaron as a concrete model . . . 15

A Appendix: Local Density Approximation (LDA) and Semiclassical Criteria **16**
- A.1 What LDA assumes: local uniformity . . . 16
- A.2 General scale separation: a unified criterion . . . 16
- A.3 LDA for ideal (or Fermi-liquid) fermions in a trap . . . 17
- A.4 LDA for weakly interacting Bose condensates (TF as LDA) . . . 17
- A.5 Local equilibrium and when LDA fails . . . 18

1 Fermi Distribution in the Uniform Ideal Fermi Gas

1.1 Fermi sea, occupation numbers, and excitations

Plane waves and occupation-number characterization. For a uniform noninteracting Fermi gas, each plane-wave mode labeled by momentum $\boldsymbol{k}$ is a single-particle eigenstate. Hence any many-body eigenstate can be fully specified by the occupation numbers

$$n(\boldsymbol{k}) \in \{0, 1\}, \tag{1}$$

where the binary constraint is the Pauli principle. In thermal equilibrium it is often convenient to use the average occupation $0 \le \langle n(\boldsymbol{k}) \rangle \le 1$, denoted again by $n(\boldsymbol{k})$ by abuse of notation.

Zero-temperature ground state—-the Fermi sea.

At $T = 0$, fermions fill single-particle levels from low to high energy. For a free dispersion $\epsilon_k = \hbar^2 k^2/(2m)$, the filled region in momentum space is a sphere $|\boldsymbol{k}| < k_F$ (the Fermi sea)[1], with

$$E_F = \frac{\hbar^2 k_F^2}{2m}. \tag{2}$$

The many-body ground state is

$$|FS\rangle = \prod_{k<k_F} \hat{c}_{\boldsymbol{k}}^\dagger |0\rangle, \tag{3}$$

and the ground-state momentum distribution is a sharp step:

$$n_0(\boldsymbol{k}) = \begin{cases} 1, & k < k_F, \\ 0, & k > k_F. \end{cases} \tag{4}$$

The chemical potential μ is defined as $\mu = E_F = \frac{\hbar^2 k_F^2}{2m}$.

Particle and hole excitations, and positivity of excitation energy. Elementary excitations above $|FS\rangle$ are particle excitations and hole excitations:

$$|\boldsymbol{k}; \mathrm{p}\rangle = \hat{c}_{\boldsymbol{k}}^\dagger |FS\rangle \quad (k > k_F), \qquad |\boldsymbol{k}; \mathrm{h}\rangle = \hat{c}_{\boldsymbol{k}} |FS\rangle \quad (k < k_F). \tag{5}$$

Measured relative to the chemical potential $\mu = E_F$, their excitation energies are

$$\varepsilon_{\boldsymbol{k}}^{\mathrm{p}} = \epsilon_k - \mu \quad (k > k_F), \qquad \varepsilon_{\boldsymbol{k}}^{\mathrm{h}} = \mu - \epsilon_k \quad (k < k_F), \tag{6}$$

so both can be summarized as

$$\varepsilon_{\boldsymbol{k}} = |\epsilon_k - \mu| \ge 0. \tag{7}$$

Let $n(\boldsymbol{k})$ deviate from the ground-state distribution $n_0(\boldsymbol{k})$, and define $\delta n(\boldsymbol{k}) = n(\boldsymbol{k}) - n_0(\boldsymbol{k})$. For the ideal gas,

$$\delta E = \sum_{\boldsymbol{k}} (\epsilon_k - \mu)\, \delta n(\boldsymbol{k}). \tag{8}$$

For a particle–hole excitation, the contributions come in pairs: adding one particle above k_F and removing one below k_F, and Eq. (8) is manifestly positive because each term is positive in its respective domain.

[1] For a fixed number of fermions, k_F, is determined by the particle number N.
$N = g\frac{V}{(2\pi)^3}\int_{|\mathbf{k}|\le k_F} \mathrm{d}^3k = g\frac{V}{6\pi^2}k_F^3$, so $k_F = \left(\frac{6\pi^2}{g}\frac{N}{V}\right)^{1/3}$, where g is the spin-degeneracy.

1.2 Fermi–Dirac distribution, classical limit, and kinetic energy

Semiclassical equilibrium distribution in a uniform gas. For a uniform gas in a large box (volume V) with very large particle number N, the single-particle levels are so dense that we may replace sums by integrals, $\sum_{\boldsymbol{k}} \to V \int d^3k/(2\pi)^3$. In this *semiclassical* (continuum) description, the equilibrium average occupation of a momentum mode $\boldsymbol{k}$ is the Fermi–Dirac distribution

$$f(\boldsymbol{k}) = \frac{1}{e^{\beta(\epsilon_k - \mu)} + 1}, \qquad \epsilon_k = \frac{\hbar^2 k^2}{2m}, \qquad \beta = \frac{1}{k_B T}, \tag{9}$$

where μ is fixed by the number constraint $N = \sum_{\boldsymbol{k}} f(\boldsymbol{k})$.

Zero-temperature limit. Let $x = \beta(\epsilon_k - \mu)$. As $T \to 0$ we have $\beta \to \infty$, so

$$\lim_{\beta\to\infty} \frac{1}{e^{\beta(\epsilon_k-\mu)} + 1} = \begin{cases} 1, & \epsilon_k < \mu, \\ 0, & \epsilon_k > \mu, \end{cases} \tag{10}$$

i.e. $f(\boldsymbol{k}) \to \Theta(\mu - \epsilon_k)$. Defining the Fermi energy $E_F \equiv \mu(T = 0)$ and Fermi momentum k_F by

$$E_F = \frac{\hbar^2 k_F^2}{2m}, \tag{11}$$

the distribution becomes the sharp Fermi sea:

$$f(\boldsymbol{k}) \xrightarrow[T\to 0]{} \Theta(k_F - k). \tag{12}$$

Number density. In the semiclassical limit, the number density $n \equiv N/V$ is

$$n = \int \frac{d^3k}{(2\pi)^3} f(\boldsymbol{k}). \tag{13}$$

At $T = 0$, using Eq. (12) one gets

$$n = \int_{k<k_F} \frac{d^3k}{(2\pi)^3} = \frac{1}{(2\pi)^3} 4\pi \int_0^{k_F} k^2\, dk = \frac{k_F^3}{6\pi^2}, \tag{14}$$

which can be inverted as $k_F = (6\pi^2 n)^{1/3}$.

Fermi temperature. A Fermi gas behaves classically in the high-temperature and dilute regime, where quantum degeneracy effects are negligible, and the relevant energy scale separating classical and quantum behavior is set by the Fermi temperature:

$$T_F \equiv \frac{E_F}{k_B} = \frac{\hbar^2 k_F^2}{2mk_B}. \tag{15}$$

This T_F sets the crossover between classical and degenerate regimes.

Classical (Maxwell–Boltzmann) limit and its condition

The relevant criterion is not "high temperature" by itself, but *low phase-space occupancy*: the average occupation per phase-space cell is much smaller than unity. Two equivalent characterizations are:

(A) Small fugacity. Define the fugacity $z \equiv e^{\beta\mu}$. The nondegenerate regime is $z \ll 1$.

(B) Thermal de Broglie wavelength criterion. In 3D,

$$\lambda_T \equiv \sqrt{\frac{2\pi\hbar^2}{mk_BT}}, \tag{16}$$

and the nondegenerate regime is $n\lambda_T^3 \ll 1$, where $n = N/V$ is the number density.

Deriving the Maxwell–Boltzmann form from $z \ll 1$. For a uniform ideal Fermi gas,

$$f(\epsilon) = \frac{1}{e^{\beta(\epsilon-\mu)}+1} = \frac{1}{z^{-1}e^{\beta\epsilon}+1}. \tag{17}$$

If $z \ll 1$, then $z^{-1}e^{\beta\epsilon} \gg 1$ for all $\epsilon \geq 0$, and

$$f(\epsilon) = \frac{1}{z^{-1}e^{\beta\epsilon}} \cdot \frac{1}{1+ze^{-\beta\epsilon}} = ze^{-\beta\epsilon}\Big(1 - ze^{-\beta\epsilon} + O(z^2)\Big). \tag{18}$$

Keeping only the leading term gives the Maxwell–Boltzmann limit

$$f(\epsilon) \approx ze^{-\beta\epsilon} = e^{-\beta(\epsilon-\mu)}. \tag{19}$$

The first quantum-statistical correction is of order $O(z^2)$, so "degeneracy effects are negligible" means precisely z is small.

Equivalence $z \ll 1 \iff n\lambda_T^3 \ll 1$. Using the 3D density of states (per volume)

$$g(\epsilon) = \frac{1}{2\pi^2}\left(\frac{2m}{\hbar^2}\right)^{3/2}\sqrt{\epsilon}, \tag{20}$$

the density is

$$n = \int_0^\infty d\epsilon\, g(\epsilon)\, f(\epsilon). \tag{21}$$

In the $z \ll 1$ regime, substitute $f(\epsilon) \approx ze^{-\beta\epsilon}$ and use $\int_0^\infty d\epsilon\, \epsilon^{1/2}e^{-\beta\epsilon} = \frac{\sqrt{\pi}}{2}\beta^{-3/2}$, to obtain

$$n \approx z\left(\frac{mk_BT}{2\pi\hbar^2}\right)^{3/2} = \frac{z}{\lambda_T^3}. \tag{22}$$

Hence $z \approx n\lambda_T^3$, and therefore $z \ll 1$ is equivalent to $n\lambda_T^3 \ll 1$.

Kinetic energy. Define the kinetic energy per particle

$$E_k \equiv \frac{1}{n}\int \frac{d^3k}{(2\pi)^3}\,\epsilon_k\, f(\boldsymbol{k}). \tag{23}$$

■ **High-T limit.** In the classical limit Eq. (19), the momentum distribution is Gaussian:

$$f(\boldsymbol{k}) \propto e^{-\beta\hbar^2k^2/(2m)}. \tag{24}$$

Substituting this into Eq. (23), the prefactor z cancels between numerator and denominator, and the remaining Gaussian integrals yield

$$E_k \xrightarrow[T\gg T_F]{} \frac{3}{2}k_BT. \tag{25}$$

■ **Low-T limit.** At $T = 0$, $f(\boldsymbol{k}) = \Theta(k_F - k)$, so

$$\frac{E_k}{1} = \frac{1}{n}\int_{k<k_F} \frac{d^3k}{(2\pi)^3}\,\frac{\hbar^2k^2}{2m} = \frac{1}{n}\cdot\frac{1}{(2\pi)^3}\,4\pi\int_0^{k_F} dk\,k^2\frac{\hbar^2k^2}{2m}. \tag{26}$$

Evaluating the integral gives

$$\int_0^{k_F} dk\,k^4 = \frac{k_F^5}{5}, \qquad \Rightarrow \qquad E_k(T=0) = \frac{1}{n}\cdot\frac{\hbar^2}{2m}\cdot\frac{4\pi}{(2\pi)^3}\cdot\frac{k_F^5}{5} = \frac{3}{5}\frac{\hbar^2k_F^2}{2m} = \frac{3}{5}E_F, \tag{27}$$

where in the last step we used $n = k_F^3/(6\pi^2)$ from Eq. (14).

Sommerfeld expansion (result-oriented): low-T corrections

For $T \ll T_F$, only a thin shell of width $\sim k_BT$ around $\epsilon = \mu$ contributes to thermal corrections. Using the Sommerfeld expansion for Fermi integrals at fixed density n, one finds

$$\mu(T) = E_F\left[1 - \frac{\pi^2}{12}\left(\frac{T}{T_F}\right)^2 + O\left(\frac{T}{T_F}\right)^4\right], \tag{28}$$

$$E_k(T) = \frac{3}{5}E_F\left[1 + \frac{5\pi^2}{12}\left(\frac{T}{T_F}\right)^2 + O\left(\frac{T}{T_F}\right)^4\right], \tag{29}$$

and therefore the specific heat is linear:

$$\frac{C_V}{N} = \frac{\partial E_k}{\partial T} = \frac{\pi^2}{2}k_B\frac{T}{T_F} + O\left(\frac{T}{T_F}\right)^3. \tag{30}$$

1.3 External Potential and Local density approximation(LDA)

Semiclassical distribution in phase space. With a slowly varying external potential $V(\boldsymbol{r})$, the semiclassical equilibrium distribution is

$$f(\boldsymbol{r},\boldsymbol{k}) = \frac{1}{e^{\beta(\epsilon_k + V(\boldsymbol{r}) - \mu)} + 1}. \tag{31}$$

The local density follows from momentum integration:

$$n(\boldsymbol{r}) = \int \frac{d^3k}{(2\pi)^3}\,f(\boldsymbol{r},\boldsymbol{k}), \qquad N = \int d^3r\,n(\boldsymbol{r}). \tag{32}$$

This is the LDA statement: a trapped system is treated as locally uniform with a local chemical potential

$$\mu(\boldsymbol{r}) = \mu - V(\boldsymbol{r}). \tag{33}$$

Zero-temperature Case: $n(\boldsymbol{r}) \propto (\mu - V)^{3/2}$.

At $T = 0$, Eq. (31) becomes $f = \Theta(\mu - V - \epsilon_k)$, defining a local Fermi momentum

$$\frac{\hbar^2k_F^2(\boldsymbol{r})}{2m} = \mu - V(\boldsymbol{r}), \qquad k_F(\boldsymbol{r}) = 0 \ \text{ if } \ \mu < V(\boldsymbol{r}). \tag{34}$$

For a single spin component,

$$n(\boldsymbol{r}) = \frac{k_F^3(\boldsymbol{r})}{6\pi^2} = \frac{1}{6\pi^2}\left(\frac{2m}{\hbar^2}\right)^{3/2}\Big(\mu - V(\boldsymbol{r})\Big)^{3/2}\Theta\Big(\mu - V(\boldsymbol{r})\Big). \tag{35}$$

Review: Thomas–Fermi (TF) profile for a weakly interacting Bose condensate and its link to LDA

For a dilute Bose condensate with contact interaction (contact term) $g_B = 4\pi\hbar^2 a_B/m_B$, the zero-temperature condensate is described at mean-field level by the Gross–Pitaevskii (GP) energy functional

$$E[\psi] = \int d^3r \left[\frac{\hbar^2}{2m_B} |\nabla\psi(\boldsymbol{r})|^2 + V(\boldsymbol{r})|\psi(\boldsymbol{r})|^2 + \frac{g_B}{2}|\psi(\boldsymbol{r})|^4 \right], \qquad n_B(\boldsymbol{r}) \equiv |\psi(\boldsymbol{r})|^2. \tag{36}$$

Minimizing $E[\psi] - \mu_B \int d^3r\, |\psi|^2$ yields the stationary GP equation

$$\left[-\frac{\hbar^2}{2m_B}\nabla^2 + V(\boldsymbol{r}) + g_B n_B(\boldsymbol{r}) \right] \psi(\boldsymbol{r}) = \mu_B\, \psi(\boldsymbol{r}). \tag{37}$$

The Thomas–Fermi (TF) approximation neglects the kinetic ("quantum pressure") term $-(\hbar^2/2m_B)\nabla^2\psi$, which is valid when the density varies slowly on the healing-length scale. Then Eq. (37) reduces to the local algebraic relation

$$\mu_B = V(\boldsymbol{r}) + g_B n_B(\boldsymbol{r}), \tag{38}$$

so the density profile is

$$n_B(\boldsymbol{r}) = \frac{\mu_B - V(\boldsymbol{r})}{g_B}\, \Theta\big(\mu_B - V(\boldsymbol{r})\big). \tag{39}$$

Connection to LDA. Equation (38) is precisely an LDA statement: one uses the *uniform* equation of state for a weakly interacting condensate, $\mu_B = g_B n$, and replaces the global chemical potential by a local one,

$$\mu_B \;\mapsto\; \mu_B(\boldsymbol{r}) \equiv \mu_B - V(\boldsymbol{r}), \qquad n_B(\boldsymbol{r}) = \frac{\mu_B(\boldsymbol{r})}{g_B}\, \Theta\big(\mu_B(\boldsymbol{r})\big). \tag{40}$$

The manifestation is **neglecting the quantum pressure term**, which holds when the density varies slowly on the healing-length scale.

Boson vs Fermion. The formal similarity to the trapped ideal-fermion result $n(\boldsymbol{r}) \propto (\mu - V)^{3/2}$ hides different physics: TF for bosons follows from interaction–potential balance in GP theory, whereas ideal fermions are controlled by kinetic (Pauli) pressure through the fermionic equation of state.

1.4 Example: Harmonic Trap

Trap geometry and the notion of a "cloud". Consider an anisotropic harmonic trap

$$V(\boldsymbol{r}) = \frac{m}{2}\left(\omega_x^2 x^2 + \omega_y^2 y^2 + \omega_z^2 z^2\right), \qquad \bar{\omega} = (\omega_x\omega_y\omega_z)^{1/3}. \tag{41}$$

At $T = 0$, the density is supported where $\mu > V(\boldsymbol{r})$. The resulting spatial distribution $n(\boldsymbol{r})$ is the "cloud". The typical radii R_i (edge positions) are defined by $V(R_i\hat{e}_i) = \mu$:

$$R_i = \sqrt{\frac{2\mu}{m\omega_i^2}}, \qquad i = x, y, z. \tag{42}$$

Explicit integration for $N(\mu)$ and $\mu(N)$. Using Eq. (35) with the harmonic potential gives an

exact semiclassical relation between N and μ:

$$\mu = (6N)^{1/3}\hbar\bar{\omega}. \tag{43}$$

Derivation of $\mu = (6N)^{1/3}\hbar\bar{\omega}$ for one spin component

Start from Eq. (35) and integrate over the ellipsoid $\mu > V(\boldsymbol{r})$. Introduce scaled coordinates $u_i = x/R_x$, etc., so that

$$V(\boldsymbol{r}) = \mu(u_x^2 + u_y^2 + u_z^2), \qquad d^3r = R_xR_yR_z\, d^3u, \qquad R_xR_yR_z = \frac{(2\mu)^{3/2}}{m^{3/2}\omega_x\omega_y\omega_z}. \tag{44}$$

Then

$$N = \int d^3r\, n(\boldsymbol{r}) = \frac{1}{6\pi^2}\left(\frac{2m}{\hbar^2}\right)^{3/2} R_xR_yR_z\, \mu^{3/2} \int_{u<1} d^3u\, (1-u^2)^{3/2}. \tag{45}$$

The remaining integral is isotropic:

$$\int_{u<1} d^3u\, (1-u^2)^{3/2} = 4\pi \int_0^1 du\, u^2(1-u^2)^{3/2} = \frac{\pi^2}{8}. \tag{46}$$

Combining everything yields

$$N = \frac{1}{6}\left(\frac{\mu}{\hbar\bar{\omega}}\right)^3, \qquad \Rightarrow \qquad \mu = (6N)^{1/3}\hbar\bar{\omega}. \tag{47}$$

1.5 Time-of-flight (TOF): momentum distribution and aspect ratio

Momentum distribution from LDA. Define the momentum distribution by integrating the phase-space distribution over space:

$$n(\boldsymbol{k}) = \int d^3r\, f(\boldsymbol{r}, \boldsymbol{k}). \tag{48}$$

In LDA for a noninteracting trapped gas, the dependence on $\boldsymbol{k}$ enters only through ϵ_k, hence $n(\boldsymbol{k})$ is isotropic even if the trap is anisotropic.

Ballistic TOF mapping and aspect ratio. After release from the trap, if interactions during expansion are negligible (collisionless regime), the long-time density profile maps to the momentum distribution:

$$n(\boldsymbol{r}, t) \simeq \left(\frac{m}{\hbar t}\right)^3 n\left(\boldsymbol{k} = \frac{m\boldsymbol{r}}{\hbar t}\right). \tag{49}$$

Thus an initially anisotropic real-space cloud can evolve into an isotropic profile at long times because $n(\boldsymbol{k})$ is isotropic; the aspect ratio approaches unity.

Hydrodynamic contrast (experimental diagnostic). If the gas exhibits hydrodynamic expansion (due to strong collisions or superfluidity), the velocity field is anisotropic and the expansion can remain anisotropic, sometimes showing inversion of the aspect ratio. This contrast is widely used to distinguish ballistic (nearly free) behavior from hydrodynamic behavior in experiments.

2 Quantized Conductance through a Quantum Point Contact

Why study QPC transport?. Transport accesses the low-energy structure of fermions in a complementary way to thermodynamics. A two-terminal geometry provides a clean near-

equilibrium probe where the current is controlled by (i) the energy window set by $\mu_L - \mu_R$ and (ii) the transmission of discrete transverse channels in the constriction.

2.1 Two-terminal setup and the Landauer–Büttiker formula

Two reservoirs and the bias window. Consider two large reservoirs (left/right) connected by a narrow channel. Each reservoir is in (quasi-)equilibrium with chemical potentials $\mu_L > \mu_R$. Particles contribute to left-to-right current if a state is occupied on the left but empty on the right, which is encoded by $f(E, \mu_L) - f(E, \mu_R)$.

Landauer–Büttiker current. A convenient form for the particle current is

$$I = \sum_n \int dE\, v(E)\, g(E)\, T_n(E) \Big[f(E, \mu_L) - f(E, \mu_R) \Big], \tag{50}$$

where n labels channels (transverse modes), $T_n(E)$ is the transmission coefficient, $v(E)$ is the group velocity along the transport direction, and $g(E)$ is the density of states (DOS) per energy for that channel.

Physical meaning of the Landauer–Büttiker current formula

Equation (50) is a *phase-space (or energy-resolved) counting* of how many particles per unit time successfully traverse the constriction.

Flux = (states per energy) × (velocity) × (occupation imbalance). Fix a channel n and an energy window $[E, E + dE]$. The one-dimensional DOS $g(E)$ tells you how many *available* propagating states in that channel lie in this window (per unit energy). Each such state carries particles with group velocity $v(E)$ along the transport direction. Therefore $v(E)\, g(E)\, dE$ has the meaning of a *particle flux capacity* of that channel within $[E, E + dE]$ (how many particles per unit time could be carried if those states were occupied).
The actual net transport is controlled by the occupancy difference between the left and right reservoirs. The factor $f(E, \mu_L) - f(E, \mu_R)$ measures the *net imbalance of filled incoming states*: states at energy E that are occupied on the left but not on the right contribute to flow from left to right (and vice versa). In particular, at low T this difference restricts transport to the energy window between μ_R and μ_L.
Finally, the constriction is not perfectly transparent in general. The transmission $T_n(E) \in [0, 1]$ is the probability that an incoming particle at energy E in channel n makes it through without being reflected. Multiplying by $T_n(E)$ converts the *incoming flux* into the *transmitted flux*.
Putting these ingredients together and summing over channels gives Eq. (50):

$$\text{current} = \sum_n \int dE \quad \underbrace{v(E)g(E)}_{\substack{\text{flux per energy} \\ \text{for channel } n}} \quad \underbrace{T_n(E)}_{\text{transmission}} \quad \underbrace{\Big[f_L(E) - f_R(E) \Big]}_{\text{occupation imbalance}} .$$

Dimensional check. If $g(E)$ is defined as "number of states per energy" for a 1D channel, then $g(E) \sim 1/\text{energy}$, and $v(E)g(E) \sim (\text{length/time}) \cdot (1/\text{energy})$. With the conventional normalization of 1D states, the product $v(E)g(E)$ becomes an energy-independent constant $1/h$ (shown explicitly in the next subsection), so that the integral $\int dE\, (\cdots)$ yields a rate (particles per unit time), as required for I.

1D simplification: deriving $v(E)$ and $g(E)$. In one dimension, with dispersion $E(k)$,

$$v(E) = \frac{1}{\hbar} \frac{dE}{dk}. \tag{51}$$

The 1D DOS per unit length is obtained by state counting: the number of states in $[k, k+dk]$ per length is $(2\pi)^{-1}dk$, so

$$g(E) = \frac{1}{2\pi}\left|\frac{dk}{dE}\right| = \frac{1}{2\pi}\left|\frac{dE}{dk}\right|^{-1}. \tag{52}$$

Therefore,

$$v(E)\, g(E) = \frac{1}{2\pi\hbar} = \frac{1}{h}. \tag{53}$$

Substituting into Eq. (50) yields

$$I = \frac{1}{h}\sum_n \int dE\, T_n(E)\Big[f(E,\mu_L) - f(E,\mu_R)\Big]. \tag{54}$$

2.2 QPC design and semiclassical channel picture

QPC potential and the engineering target. A QPC is engineered so that transmission is nearly ballistic[2] for open channels. In cold atoms, a typical model potential (transport along $\hat{y}$) is

$$V_{\mathrm{QPC}}(\boldsymbol{r}) = \frac{m}{2}\omega_z^2(y)z^2 + \frac{m}{2}\omega_x^2(y)x^2 - V_g f_g(y), \tag{55}$$

with localized confinements $\omega_z(y) = \omega_z^0 e^{-y^2/l_z^2}$, $\omega_x(y) = \omega_x^0 e^{-y^2/l_x^2}$, and a gate $f_g(y) = e^{-y^2/l_g^2}$. Typically $l_z > l_x$, so the channel is first squeezed into quasi-2D and then quasi-1D near $y = 0$.

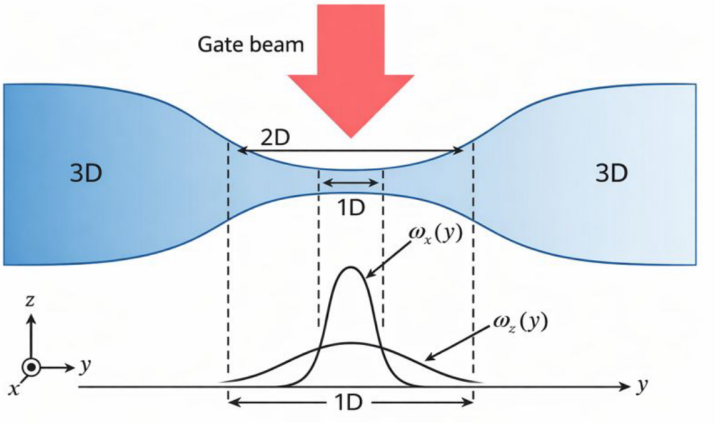

Adiabatic separation: from 3D to effective 1D channel potentials. The central semiclassical step is to treat the longitudinal direction y as "slow" and transverse directions (x, z) as "fast".

Separation of variables and where mode-mixing comes from

Consider a single-particle Schrödinger equation with Hamiltonian $\hat{H} = \hat{p}^2/(2m) + V_{\mathrm{QPC}}(\boldsymbol{r})$. At fixed y, the transverse Hamiltonian is a 2D harmonic oscillator:

$$\hat{H}_\perp(y) = \frac{\hat{p}_x^2 + \hat{p}_z^2}{2m} + \frac{m}{2}\omega_x^2(y)x^2 + \frac{m}{2}\omega_z^2(y)z^2 - V_g f_g(y), \tag{56}$$

with eigenstates $\phi_{mn}(x, z; y)$ and eigenvalues

$$V_{mn}(y) = \left(m + \frac{1}{2}\right)\hbar\omega_z(y) + \left(n + \frac{1}{2}\right)\hbar\omega_x(y) - V_g f_g(y). \tag{57}$$

[2]Here ballistic means there is almost no scattering, *i.e.* $T_n = 1$

Expand the full wavefunction as $\Psi(x, y, z) = \sum_{mn} \phi_{mn}(x, z; y)\, \varphi_{mn}(y)$. Plugging back produces an effective multi-channel 1D equation in y with:

1. **Diagonal terms** $V_{mn}(y)$ (channel potentials), and
2. **Off-diagonal couplings** $\langle m'n'|\partial_y|mn\rangle$ and $\langle m'n'|\partial_y^2|mn\rangle$, which mix channels.

Thus "inter-channel scattering" means transitions $mn \to m'n'$ induced by the y-dependence of ϕ_{mn}. It is suppressed when $\omega_x(y), \omega_z(y)$ vary slowly so that these derivative matrix elements are small compared with channel energy separations and the longitudinal kinetic scale.

Discrete channels and smoothness against backscattering. Because $V_{mn}(y)$ is peaked near $y = 0$, each channel resembles a smooth barrier. Backscattering is suppressed if the barrier varies slowly on the Fermi-wavelength scale of incoming particles near the reservoirs. A convenient criterion (schematic but practical) is

$$\left\langle \frac{\partial_y^2 V_{mn}(y)}{V_{mn}(y)} \right\rangle \ll k_F^2, \tag{58}$$

so that the potential does not efficiently couple forward- to backward-propagating states.

Three design principles (summary).

1. **1D transport** so that $v(E)g(E) = 1/h$.
2. **Discrete modes** with transverse level spacing larger than $k_B T$ (otherwise steps are thermally smeared).
3. **Suppressed backscattering / mode-mixing** via a smooth longitudinal profile and slow variation of $\omega_x(y), \omega_z(y)$.

2.3 Conductance quantization

Open vs closed channels and step-like transmission. In an ideal QPC, transmission is nearly unity once a channel is energetically open and nearly zero otherwise:

$$T_{mn}(E) \approx \Theta\Big(E - V_{mn}(0)\Big). \tag{59}$$

Channels with $E > V_{mn}(0)$ are open; those with $E < V_{mn}(0)$ are closed.

Zero-temperature derivation. At $T = 0$, $f(E, \mu) = \Theta(\mu - E)$. Insert Eq. (59) into Eq. (54):

$$I = \frac{1}{h} \sum_{mn} \int dE\, \Theta(E - V_{mn}(0)) \Big[\Theta(\mu_L - E) - \Theta(\mu_R - E)\Big]. \tag{60}$$

The product of step functions restricts E to the window $\mu_R < E < \mu_L$ for each open channel (assuming $\mu_{L,R}$ lie above the channel threshold). Thus each open channel contributes exactly $\Delta\mu = \mu_L - \mu_R$:

$$\int dE \Big[\Theta(\mu_L - E) - \Theta(\mu_R - E)\Big] = \mu_L - \mu_R \equiv \Delta\mu, \tag{61}$$

and therefore

$$I = \frac{\Delta\mu}{h} N_{\text{open}}, \qquad G \equiv \frac{I}{\Delta\mu} = \frac{1}{h} N_{\text{open}}. \tag{62}$$

■ **Quantized conductance through a QPC.** If the channel is effectively 1D, transverse modes are discrete, and backscattering is suppressed so that open channels have $T \simeq 1$, then at $T = 0$

$$G = \frac{1}{h} N_{\text{open}}. \tag{63}$$

At finite temperature the steps are broadened by the Fermi functions in the reservoirs.

3 Landau Fermi Liquid: Quasiparticles, m^*, Z, and Self-Energy

3.1 Core assumptions and the role of the Fermi surface

What is generalized from the ideal gas?. The ideal Fermi gas suggests a robust organizing structure: the Fermi surface. Landau's hypothesis is that in a broad class of interacting fermion systems, low-energy excitations remain in one-to-one correspondence with those of the ideal gas, but with renormalized parameters.

Two defining features of a Fermi liquid. A (uniform) Fermi liquid is characterized by:

1. **A discontinuity in $n_0(\boldsymbol{k})$ at the Fermi surface:**

$$Z \equiv n_0(k_F^-) - n_0(k_F^+), \qquad 0 < Z < 1. \tag{64}$$

2. **Gapless excitations at the Fermi surface:** the quasiparticle energy measured from μ satisfies $|\mathcal{E}_{\boldsymbol{k}} - \mu| \to 0$ as $k \to k_F$.

These are not independent accidents: they are tied to the existence of a quasiparticle pole in the single-particle Green's function.

3.2 Why quasi-particles exist

Single-particle spectroscopy as the starting point. A sharp notion of a "quasiparticle" is most cleanly formulated via the (retarded) single-particle Green's function and its spectral function. We write the Dyson form

$$G(\boldsymbol{k}, \omega) = \frac{1}{\omega - \xi_k - \Sigma(\boldsymbol{k}, \omega)}, \qquad \xi_k \equiv \epsilon_k - \mu, \qquad \epsilon_k = \frac{\hbar^2 k^2}{2m}, \tag{65}$$

where $\Sigma(\boldsymbol{k}, \omega)$ is the (retarded) self-energy, generally complex: $\Sigma = \operatorname{Re}\Sigma + i \operatorname{Im}\Sigma$. The spectral function is

$$A(\boldsymbol{k}, \omega) \equiv -\frac{1}{\pi} \operatorname{Im} G(\boldsymbol{k}, \omega), \tag{66}$$

which is the quantity directly accessed by single-particle spectroscopy (ARPES in solids; rf spectroscopy in cold atoms).

A *quasiparticle* exists near the Fermi surface if, for $\boldsymbol{k}$ close to k_F and ω close to 0 (measured from μ), the spectral function $A(\boldsymbol{k}, \omega)$ contains a **narrow peak** whose peak position disperses smoothly with $\boldsymbol{k}$. The peak width is the inverse lifetime of the excitation.

Fermi-liquid hypothesis: pole + incoherent background. The Fermi-liquid assumption is that at low energy the Green's function can be decomposed as

$$G(\boldsymbol{k}, \omega) \approx \frac{Z}{\omega - \xi_{\boldsymbol{k}}^* + i0^+} + G_{\text{inc}}(\boldsymbol{k}, \omega), \tag{67}$$

where $\xi_k^* \equiv \mathcal{E}_k - \mu$ is the quasiparticle dispersion, $Z \in (0,1)$ is the pole weight, and G_{inc} is a smooth "incoherent" contribution associated with multi-particle continua. Only the pole term can produce a discontinuity in $n(\boldsymbol{k})$; a smooth G_{inc} contributes only continuous background.

Why Z is literally a residue (and why it controls the jump in $n(\boldsymbol{k})$)

At fixed $\boldsymbol{k}$, the quasiparticle pole is a simple pole of $G(\boldsymbol{k},\omega)$ in the complex ω-plane. Its coefficient is the complex-analysis residue:

$$Z = \lim_{\omega \to \xi_k^*} (\omega - \xi_k^*)\, G(\boldsymbol{k},\omega). \tag{68}$$

Because a simple pole corresponds to a δ-like coherent contribution in $A(\boldsymbol{k},\omega)$, it is precisely this coherent part that generates the jump of the momentum distribution at k_F; the incoherent part is broadened in ω and therefore yields only a smooth contribution to $n(\boldsymbol{k})$.

Stability: why the spectral peak becomes sharp at low energy. The linewidth of the quasiparticle peak is controlled by the imaginary part of the self-energy. Near the pole, one finds parametrically $\Gamma(\boldsymbol{k},\omega) \sim -Z\,\mathrm{Im}\,\Sigma(\boldsymbol{k},\omega)$, so a small $|\mathrm{Im}\,\Sigma|$ implies a long lifetime. A defining dynamical property of a Fermi liquid is that at low energy

$$\mathrm{Im}\,\Sigma(\boldsymbol{k}_F,\omega) \propto -\omega^2 - (\pi k_B T)^2, \tag{69}$$

so $\Gamma \to 0$ as $\omega \to 0$ and $T \to 0$. Physically, decay processes of a low-energy excitation require available final states near the Fermi surface, but Pauli blocking strongly restricts this phase space; the resulting phase-space suppression leads to the quadratic scaling in Eq. (69).

From the pole to Landau's energy functional. Landau's phenomenology can be viewed as a controlled coarse-graining of these long-lived excitations: one introduces a smooth occupation function $n(\boldsymbol{k})$ for quasiparticles and considers low-energy distortions supported in a thin shell around k_F. The energy change admits an expansion

$$\delta E = \sum_{\boldsymbol{k}} \mathcal{E}_{\boldsymbol{k}}\, \delta n(\boldsymbol{k}) + \frac{1}{2V} \sum_{\boldsymbol{k},\boldsymbol{k}'} f(\boldsymbol{k},\boldsymbol{k}')\, \delta n(\boldsymbol{k}) \delta n(\boldsymbol{k}') + \cdots, \tag{70}$$

where the linear coefficient

$$\mathcal{E}_{\boldsymbol{k}} \equiv \frac{\delta E}{\delta n(\boldsymbol{k})} \tag{71}$$

is interpreted as the quasiparticle energy.

Why the functional derivative matches "energy of adding a quasiparticle"

Microscopically, particle numbers in each $\boldsymbol{k}$ mode change in integers. However, in a macroscopic system one can construct deformations that change the occupation in a narrow region of the Fermi surface by $O(1)$ particles while spreading this change over $O(V)$ modes; the coarse-grained $\delta n(\boldsymbol{k})$ is then effectively continuous. In this sense, $\delta E/\delta n(\boldsymbol{k})$ is the energy cost *per quasiparticle* at momentum $\boldsymbol{k}$, consistent with the pole dispersion $\mathcal{E}_{\boldsymbol{k}}$ in Eq. (67).

Velocity and effective mass near the Fermi surface. Define the quasiparticle velocity from the dispersion

$$\boldsymbol{v}_{\boldsymbol{k}} = \frac{1}{\hbar} \nabla_{\boldsymbol{k}} \mathcal{E}_{\boldsymbol{k}}. \tag{72}$$

In an isotropic system, linearizing near k_F gives $\mathcal{E}_{\boldsymbol{k}} - \mu \simeq \hbar v_F (k - k_F)$, and one defines

$$v_F = \frac{\hbar k_F}{m^*}, \tag{73}$$

which sets the low-energy kinematics and (as we see next) low-T thermodynamics.

DOS at the Fermi surface and the specific heat. Low-temperature thermodynamics is controlled by excitations within an energy window $\sim k_B T$ around E_F. Therefore it is governed by the quasiparticle density of states (DOS) at the Fermi surface.

3D spherical derivation of $\mathcal{D}(E_F)$ in terms of m^*

For an isotropic dispersion $\mathcal{E}(k)$,

$$\mathcal{D}(E) := \sum_k \delta\big(E - \mathcal{E}(k)\big) = \frac{V}{(2\pi)^3} \int d^3k\, \delta\big(E - \mathcal{E}(k)\big) = \frac{V}{2\pi^2} \frac{k(E)^2}{\left|\frac{d\mathcal{E}}{dk}\right|_{k(E)}}. \tag{74}$$

At $E = E_F$, $k(E_F) = k_F$ and $\left.\frac{d\mathcal{E}}{dk}\right|_{k_F} = \hbar v_F = \hbar^2 k_F / m^*$, hence

$$\mathcal{D}(E_F) = \frac{V k_F m^*}{2\pi^2 \hbar^2}. \tag{75}$$

Using the standard low-T result for a Fermi liquid

$$C_V = \frac{\pi^2}{3} k_B^2 T\, \mathcal{D}(E_F), \tag{76}$$

one obtains

$$C_V = \frac{V k_B^2 k_F T m^*}{3\hbar^2}. \tag{77}$$

This illustrates the "universality" viewpoint: detailed interactions largely enter low-T thermodynamics through a small set of renormalized parameters (here m^*); in contrast, Z primarily controls the coherence (spectral pole weight) and the jump in $n(\boldsymbol{k})$.

3.3 Higher-order structure: quasiparticle interactions and Landau parameters

The quadratic term in Eq. (70),

$$\frac{1}{2V} \sum_{k,k'} f(\boldsymbol{k}, \boldsymbol{k}') \delta n(\boldsymbol{k}) \delta n(\boldsymbol{k}'),$$

encodes quasiparticle–quasiparticle interactions in the low-energy sector. Operationally, it determines linear-response coefficients (compressibility, spin susceptibility) and collective modes (e.g. zero sound). In an isotropic system one expands $f(\boldsymbol{k}, \boldsymbol{k}')$ on the Fermi surface in angular harmonics to define the Landau parameters, which organize interaction effects systematically beyond single-quasiparticle kinematics.

3.4 Domain of validity and possible fates of interacting Fermi systems

■ **Fermi liquid.** A stable Fermi surface with well-defined quasiparticles: finite m^* and $Z > 0$. Low-energy thermodynamics is controlled by $\mathcal{D}(E_F) \propto m^*$.

■ **Symmetry breaking (ordered phases).** Interactions may drive order (e.g. BCS pairing, density waves). Single-particle excitations can become gapped and the simple Fermi-liquid picture may no longer apply.

■ **Non-Fermi liquid.** Absence of long-lived quasiparticles (typically $Z \to 0$); the Green's function lacks a simple pole structure.

■ **Breakdown near criticality.** Approaching a transition out of a Fermi liquid, m^* can be strongly enhanced and Z can be suppressed; both trends reflect the deterioration of the quasiparticle pole.

3.5 Self-energy and the Fermi polaron as a concrete model

Self-energy relations for m^* and Z. Write the Dyson equation for the single-particle Green's function:

$$G^{-1}(\boldsymbol{p},\omega) = \omega - \epsilon_p - \Sigma(\boldsymbol{p},\omega), \qquad \epsilon_p = \frac{\hbar^2 p^2}{2m}. \tag{78}$$

Quasiparticle dispersion satisfies $\omega - \epsilon_p - \Sigma(\boldsymbol{p},\omega) = 0$. Differentiating with respect to p^2 gives the effective-mass relation at the pole:

$$\frac{m^*}{m} = \frac{1 - \frac{\partial \Sigma}{\partial \omega}}{1 + \frac{\partial \Sigma}{\partial (p^2/(2m))}}. \tag{79}$$

The residue is

$$Z^{-1} = 1 - \frac{\partial \Sigma}{\partial \omega}. \tag{80}$$

Fermi polaron: physical picture and Chevy-type variational ansatz. Consider a fully spin-polarized $\uparrow$ Fermi sea in the thermodynamic limit, plus a single $\downarrow$ impurity. The impurity interacts with $\uparrow$ fermions via s-wave contact interaction (contact term). The polaron is a dressed quasiparticle: an impurity accompanied by particle–hole excitations of the majority sea.

A minimal but accurate variational wavefunction at total momentum $\boldsymbol{p} = \boldsymbol{0}$ is

$$|\Psi\rangle_{\boldsymbol{p}=\boldsymbol{0}} = \psi_0\, \hat{c}^\dagger_{\boldsymbol{0}\downarrow}|FS\rangle + \sum_{k>k_F,\, q<k_F} \psi_{kq}\, \hat{c}^\dagger_{\boldsymbol{q}-\boldsymbol{k},\downarrow} \hat{c}^\dagger_{\boldsymbol{k}\uparrow} \hat{c}_{\boldsymbol{q}\uparrow}|FS\rangle, \tag{81}$$

with normalization $|\psi_0|^2 + \sum_{kq} |\psi_{kq}|^2 = 1$. The second term explicitly encodes the dressing cloud: the impurity excites one particle–hole pair ($\boldsymbol{q} \to \boldsymbol{k}$) and recoils to $\boldsymbol{q} - \boldsymbol{k}$ so total momentum remains zero.

What is gained by truncating to one particle–hole pair?

In principle the impurity can excite arbitrarily many particle–hole pairs. The one-pair truncation keeps the leading nontrivial dressing process while retaining a tractable closed-form self-consistency. Empirically and numerically, it captures polaron energy, m^*, and Z with high accuracy over a broad interaction range.

Contact-interaction renormalization (needed for UV finiteness). For a 3D contact interaction with coupling g, renormalization relates g to the scattering length a_s:

$$\frac{1}{g} + \frac{1}{V}\sum_{\boldsymbol{k}} \frac{1}{2\epsilon_k} = \frac{m}{4\pi\hbar^2 a_s}. \tag{82}$$

This removes ultraviolet divergences from intermediate momentum sums.

Self-consistent polaron equation and two branches. Minimizing the variational energy yields a self-consistent equation for the polaron energy $\mathcal{E}$ (at $\boldsymbol{p} = 0$) of the form

$$\mathcal{E} = \frac{1}{V}\sum_{q<k_F} \left[\frac{m}{4\pi\hbar^2 a_s} - \frac{1}{V}\sum_{\boldsymbol{k}} \frac{1}{2\epsilon_k} - \sum_{k>k_F} \frac{1}{\mathcal{E} - E_{kq}} \right]^{-1} \quad \text{(schematic structure)}, \tag{83}$$

where E_{kq} is the energy cost of creating a particle–hole pair and recoiling the impurity. The equation typically has two solutions: a negative-energy attractive polaron and a positive-energy repulsive polaron, reminiscent of lower/upper branches in the two-body problem across a scattering resonance. At unitarity $1/(k_F a_s) = 0$, $\mathcal{E}/E_F$ becomes a universal number of order unity, reflecting interaction energy comparable to kinetic energy.

Residue in the variational state. Within the ansatz Eq. (81), the weight $|\psi_0|^2$ measures how much the polaron resembles a bare impurity without disturbing the Fermi surface. Since particle–hole excitations smear the discontinuity, one identifies

$$Z = |\psi_0|^2, \tag{84}$$

consistent with the general pole-residue relation Eq. (80) when the same approximation is used to compute $\Sigma(\boldsymbol{p}, \omega)$.

A Appendix: Local Density Approximation (LDA) and Semiclassical Criteria

A.1 What LDA assumes: local uniformity

Basic statement. LDA treats an inhomogeneous trapped system as a patchwork of locally uniform systems. For any uniform equation-of-state relation $X_{\text{uni}}(\mu, T, \dots)$ (e.g. density, pressure, compressibility), LDA prescribes

$$\mu(\boldsymbol{r}) \equiv \mu - V(\boldsymbol{r}), \qquad X(\boldsymbol{r}) \approx X_{\text{uni}}\Big(\mu(\boldsymbol{r}), T, \dots\Big). \tag{85}$$

The number constraint closes the problem:

$$N = \int d^3 r\, n(\boldsymbol{r}). \tag{86}$$

Two layers of approximation. It is useful to separate two conceptually different steps:

1. **Semiclassical continuum:** replace discrete trap levels by phase-space integrals, e.g. $\sum_{\boldsymbol{k}} \to \int d^3k/(2\pi)^3$, valid when many levels are occupied.
2. **Local uniformity (LDA proper):** assume the external potential varies slowly so that the uniform equation of state applies with $\mu \to \mu(\boldsymbol{r})$.

A.2 General scale separation: a unified criterion

A generic "variation length". Let $L_V(\boldsymbol{r})$ denote the spatial scale over which the potential changes appreciably. A convenient local definition is

$$L_V(\boldsymbol{r}) \equiv \left| \frac{V(\boldsymbol{r})}{\nabla V(\boldsymbol{r})} \right|, \tag{87}$$

to be interpreted as an order-of-magnitude measure (one can use other equivalent definitions depending on context).

Microscopic length scales. LDA requires $L_V(\boldsymbol{r})$ to be much larger than the microscopic length governing the local many-body physics:

$$L_V(\boldsymbol{r}) \gg \ell_{\text{micro}}(\boldsymbol{r}). \tag{88}$$

What counts as ℓ_{micro} depends on the system:

1. ideal/weakly interacting fermions: $\ell_{\text{micro}} \sim k_F(\boldsymbol{r})^{-1}$ (local Fermi wavelength scale);
2. weakly interacting Bose condensate: $\ell_{\text{micro}} \sim \xi(\boldsymbol{r})$ (healing length).

Heuristic meaning of ℓ_{micro}

ℓ_{micro} is the distance below which the system can no longer be regarded as locally uniform. For fermions it is tied to the sharp momentum-space structure near the Fermi surface; for a condensate it is the length over which the order parameter heals and gradients cost kinetic energy (quantum pressure).

A.3 LDA for ideal (or Fermi-liquid) fermions in a trap

Semiclassical phase-space distribution. For a weakly interacting normal Fermi system (including a Fermi liquid), the semiclassical distribution is

$$f(\boldsymbol{r},\boldsymbol{k}) = \frac{1}{e^{\beta(\epsilon_k+V(\boldsymbol{r})-\mu)}+1}, \qquad n(\boldsymbol{r}) = \int \frac{d^3k}{(2\pi)^3} f(\boldsymbol{r},\boldsymbol{k}). \tag{89}$$

At $T=0$, this becomes $f=\Theta(\mu - V - \epsilon_k)$, defining the local Fermi momentum

$$\frac{\hbar^2 k_F^2(\boldsymbol{r})}{2m} = \mu - V(\boldsymbol{r}), \qquad n(\boldsymbol{r}) = \frac{k_F^3(\boldsymbol{r})}{6\pi^2} \ \text{(single spin)}. \tag{90}$$

Local length scale for fermions. A practical fermionic criterion is

$$k_F(\boldsymbol{r})\, L_V(\boldsymbol{r}) \gg 1, \tag{91}$$

equivalently $L_V \gg \lambda_F$ with $\lambda_F(\boldsymbol{r}) \sim 2\pi/k_F(\boldsymbol{r})$. This ensures that the potential does not significantly mix nearby plane-wave components over one local de Broglie wavelength, so a local momentum label remains meaningful.

Finite temperature: replace k_F^{-1} by the thermal de Broglie wavelength when appropriate

When the system is nondegenerate, the relevant microscopic length is the thermal de Broglie wavelength

$$\lambda_T = \sqrt{\frac{2\pi\hbar^2}{m k_B T}}. \tag{92}$$

A convenient condition for semiclassical treatment is $L_V \gg \lambda_T$. In the degenerate regime $T \ll T_F$, the Fermi scale k_F^{-1} is typically the more stringent one.

Semiclassical (many-level) condition in a harmonic trap. For a 3D harmonic trap with geometric mean $\bar{\omega}$, the level spacing scale is $\hbar\bar{\omega}$. A common sufficient condition for using continuum integrals is

$$\mu \gg \hbar\bar{\omega} \qquad \text{or} \qquad k_B T \gg \hbar\bar{\omega}, \tag{93}$$

which guarantees many occupied single-particle levels.

A.4 LDA for weakly interacting Bose condensates (TF as LDA)

From GP to a local equation of state. At $T=0$, the stationary GP equation reads

$$\left[-\frac{\hbar^2}{2m_B}\nabla^2 + V(\boldsymbol{r}) + g_B n_B(\boldsymbol{r})\right]\psi(\boldsymbol{r}) = \mu_B\,\psi(\boldsymbol{r}), \qquad n_B(\boldsymbol{r}) = |\psi(\boldsymbol{r})|^2. \tag{94}$$

Neglecting the kinetic (quantum pressure) term produces the Thomas–Fermi relation

$$\mu_B = V(\boldsymbol{r}) + g_B n_B(\boldsymbol{r}) \quad \Rightarrow \quad n_B(\boldsymbol{r}) = \frac{\mu_B - V(\boldsymbol{r})}{g_B}\,\Theta\big(\mu_B - V(\boldsymbol{r})\big), \tag{95}$$

which is exactly LDA using the uniform condensate equation of state $\mu_B = g_B n$ with $\mu_B(\boldsymbol{r}) = \mu_B - V(\boldsymbol{r})$.

Bosonic microscopic length: healing length. The TF/LDA step neglects gradients. The scale controlling gradient importance is the healing length

$$\xi(\boldsymbol{r}) \equiv \frac{\hbar}{\sqrt{2m_B g_B n_B(\boldsymbol{r})}}. \tag{96}$$

A practical TF/LDA validity criterion is

$$L_V(\boldsymbol{r}) \gg \xi(\boldsymbol{r}), \tag{97}$$

so the condensate density varies slowly compared with the distance over which the order parameter can heal.

A.5 Local equilibrium and when LDA fails

Hydrodynamic vs collisionless is a separate issue. LDA is an *equilibrium* (or quasi-equilibrium) approximation for static profiles and thermodynamics. Whether the gas expands hydrodynamically or ballistically after release concerns collision rates and transport, and is logically independent from LDA.

Common failure modes. LDA can fail when:

1. the system occupies only few trap levels ($\mu \sim \hbar\bar{\omega}$ and $k_B T \sim \hbar\bar{\omega}$);
2. the potential varies on microscopic scales ($L_V \not\gg \ell_{\text{micro}}$);
3. sharp interfaces or strong gradients appear (e.g. near edges where $k_F(\boldsymbol{r}) \to 0$ or where $\xi(\boldsymbol{r})$ becomes large);
4. the system is far from local equilibrium (strong nonequilibrium gradients, fast driving).

Edge regions and "turning points"

Near the classical turning point where $\mu \approx V(\boldsymbol{r})$, the local Fermi momentum $k_F(\boldsymbol{r})$ becomes small and the fermionic criterion $k_F L_V \gg 1$ can break down even if it is well satisfied in the bulk. Similarly, for bosons the healing length $\xi(\boldsymbol{r})$ grows when $n_B(\boldsymbol{r})$ is small, so TF/LDA fails first near the edges.